Research in Astronomy and Astrophysics, 24:085012 (6pp), 2024 August https://doi.org/10.1088/1674-4527/ad63e6

Charged Particles Capture Cross-section by a Weakly Charged Schwarzschild Black Hole

A. M. Al Zahrani and A. Al-Jama
Physics Department, King Fahd University of Petroleum and Minerals, Dhahran 31261, Saudi Arabia; amz@kfupm.edu.sa, ahmad.aljama1905@gmail.com
Received 2024 June 7; revised 2024 July 6; accepted 2024 July 15; published 2024 August 7

Abstract

We study the capture cross-section of charged particles by a weakly charged Schwarzschild black hole. The dependence of the maximum impact parameter for capture on the particle's energy is investigated numerically for different values of the electromagnetic coupling strength between the particle and the black hole. The capture cross-section is then calculated. We show that the capture cross-section is independent of the electromagnetic coupling for ultra-relativistic particles. The astrophysical implications of our results are discussed.

Key words: stars: black holes – accretion – accretion disks – black hole physics

1. Introduction

Studying the capture cross-section of black holes is central to understanding how matter interacts with them. It helps us understand the process of matter accretion by a black hole which in turn determines how its mass, angular momentum and charge evolve. It can also help us understand the environment near black holes. Moreover, scrutinizing capture cross-section can be used to test theories of gravity in strong gravitational fields.

Astrophysicists generally assume black holes are electrically neutral. This is because they would quickly attract oppositely charged matter to balance out any access charge. However, there are compelling reasons why weakly charged black holes might exist as discussed in Al Zahrani (2021, 2022), Zajaček & Tursunov (1904), Zajaček et al. (2019, 2018), Carter (1973) and the references therein. The differences in how a black hole accretes electrons and protons within its plasma environment, influenced by radiation, could render it charged. Also, the spin of a black hole in the presence of a magnetic field can induce the accretion of charged particles. In fact, using the Event Horizon Telescope (EHT) observations, it was inferred that Sgr A* and M87 can be charged (Ghosh & Afrin 2023; Kocherlakota et al. 2021). The black hole's charge is weak in the sense that it has no tangible effect on spacetime, but its effect on charged particle dynamics is prominent.

There are numerous astrophysical scenarios wherein charged particles are drawn into black holes. Stars within the Roche limits near black holes often contribute matter through tidal interactions. Additionally, stars emit streams of charged particles as stellar winds. Highly energetic charged particles, resulting from supernovae, gamma-ray bursts, and bipolar jets from compact objects, frequently find their way into the vicinity of black holes. These processes collectively enrich the environment around black holes with a significant population of charged particles.

The concept of capture cross-sections has been explored extensively for various black hole types. Foundational treatment which examines photon and neutral particle capture by Schwarzschild black holes was given in several monographs, such as Frolov & Zelnikov (2011). Further work addressed capture cross-sections of charged and neutral particles by Kerr-Newman black holes, including the implications for black hole spin and charge evolution (Young 1976). Capture by Reissner–Nordström black holes was also investigated (Zakharov 1994). In the context of higher-dimensional black holes, studies have focused on calculating photon critical impact parameters for Schwarzschild–Tangherlini black holes (Connell & Frolov 2008; Tsukamoto et al. 2014; Singh & Ghosh 2018; Bugden 2020). The capture cross-section for massive particles was determined in Ahmedov et al. (2021). Additionally, research extends to particle capture in Myers–Perry rotating spacetime which describes rotating black holes in five-dimensions (Gooding & Frolov 2008). Moreover, wave capture cross-sections have been studied for various black hole configurations (see Anacleto et al. 2023 and the references within).

In this research, we examine the capture cross-section of charged particles by a weakly charged Schwarzschild black hole and discuss the astrophysical consequences of our findings. The paper is organized as follows: In Section 2, we review the dynamics of charged particles in the background of a weakly charged black hole. We then review the capture cross-section of neutral particles in Section 3. The capture cross-section of charged particles is calculated for different coupling strengths and particle energies in Section 4. Finally, we summarize our main findings and discuss their astrophysical consequences in Section 5. We use the sign conventions

adopted in Misner et al. (1973) and geometrized units where $c = G = k = 1$, where k is the electrostatic constant.

2. Charged Particles Near a Weakly Charged Schwarzschild Black Hole

Here, we review the dynamics of charged particles near a weakly charged black hole. The spacetime geometry around a black hole of mass M and charge Q is described by the Reissner–Nordström metric which reads (Misner et al. 1973)

$$ds^2 = -hdt^2 + h^{-1}dr^2 + r^2d\theta^2 + r^2\sin^2\theta d\phi^2, \tag{1}$$

where $h = 1 - r_S/r + Q^2/r^2$ and $r_S = 2M$ is the Schwarzschild radius. The electromagnetic 4-potential is

$$A_\mu = -\frac{Q}{r}\delta^0_\mu. \tag{2}$$

However, when the charge is weak we can ignore the curvature due to it and use the Schwarzschild metric, which reads (Misner et al. 1973)

$$ds^2 = -fdt^2 + f^{-1}dr^2 + r^2d\theta^2 + r^2\sin^2\theta d\phi^2, \tag{3}$$

where $f = 1 - r_S/r$. This weak charge approximation is valid unless the charge creates curvature comparable to that due to the black hole's mass. This happens when

$$Q^2 \sim M^2. \tag{4}$$

In conventional units, the weak charge approximation fails when

$$Q \sim \frac{G^{1/2}M}{k^{1/2}} \sim 10^{20}\,\frac{M}{M_\odot}\ \text{coulombs}. \tag{5}$$

This charge is way greater than the greatest estimated charge on any black hole. Although the black hole charge is tiny, its effect on charged particle dynamics is profound because it is multiplied by the charge-to-mass ratio of these particles ($\sim 10^{21}\,\mathrm{m}^{-1}$ for electrons and $\sim 10^{18}\,\mathrm{m}^{-1}$ for protons).

The Lagrangian describing a charged particle of charge q and mass m in a spacetime described by a metric $g_{\mu\nu}$ and an electromagnetic field produced by a 4-potential A^μ reads (Chandrasekhar 1983)

$$L = \frac{1}{2}mg_{\mu\nu}u^\mu u^\nu + qu^\mu A_\mu, \tag{6}$$

where $u^\mu \equiv dx^\mu/d\tau$ is the particle's 4-velocity and τ is its proper time. In our case, the Lagrangian becomes

$$L = \frac{1}{2}m\left[-f\left(\frac{dt}{d\tau}\right)^2 + f^{-1}\left(\frac{dr}{d\tau}\right)^2 + r^2\left(\frac{d\theta}{d\tau}\right)^2 + r^2\sin^2\theta\left(\frac{d\phi}{d\tau}\right)^2\right] - qQ\frac{dt}{d\tau}. \tag{7}$$

This Lagrangian is cyclic in t and ϕ, which means that the particle's energy and azimuthal angular momentum are constants of motion. The specific energy and azimuthal angular momentum are, respectively, given by

$$\mathcal{E} = -\frac{1}{m}\frac{\partial L}{\partial\left(\frac{dt}{d\tau}\right)} = f\frac{dt}{d\tau} + \frac{qQ}{mr}, \tag{8}$$

$$\ell = \frac{1}{m}\frac{\partial L}{\partial\left(\frac{d\phi}{d\tau}\right)} = r^2\sin^2\theta\frac{d\phi}{d\tau}. \tag{9}$$

Combining these equations with the normalization condition $g_{\mu\nu}u^\mu u^\nu = -1$ and solving for $dr/d\tau$ give

$$\left(\frac{dr}{d\tau}\right)^2 = \left(\mathcal{E} - \frac{qQ}{mr}\right)^2 - f\left[r^2\left(\frac{d\theta}{d\tau}\right)^2 + \frac{\ell^2}{r^2\sin^2\theta} + 1\right]. \tag{10}$$

In the equatorial plane where $\theta = \pi/2$, the equation becomes

$$\left(\frac{dr}{d\tau}\right)^2 = \left(\mathcal{E} - \frac{qQ}{mr}\right)^2 - f\left(\frac{\ell^2}{r^2} + 1\right). \tag{11}$$

Let us rewrite the last equation in a dimensionless form. We first introduce the following dimensionless quantities:

$$\mathcal{T} = \frac{\tau}{r_S}, \qquad \rho = \frac{r}{r_S}, \qquad \mathcal{L} = \frac{\ell}{r_S}. \tag{12}$$

Equation (11) then becomes

$$\left(\frac{d\rho}{d\mathcal{T}}\right)^2 = \left(\mathcal{E} - \frac{\alpha}{\rho}\right)^2 - f\left(\frac{\mathcal{L}^2}{\rho^2} + 1\right), \tag{13}$$

where

$$\alpha = \frac{qQ}{mr_S}. \tag{14}$$

The parameter α represents the relative strength of the electromagnetic force to the Newtonian gravitational force. We can rewrite Equation (13) as

$$\left(\frac{d\rho}{d\mathcal{T}}\right)^2 = (\mathcal{E} - V_+)(\mathcal{E} - V_-), \tag{15}$$

where

$$V_\pm = \frac{\alpha}{\rho} \pm \sqrt{f\left(\frac{\mathcal{L}^2}{\rho^2} + 1\right)}, \tag{16}$$

is an effective potential. It is V_+ that corresponds to physical, future-directed motion and hence will be used in all of the analyses below. Without loss of generality, we will consider $\mathcal{L} > 0$ only.

It was estimated in Zajaček et al. (2019) that the charge of Sgr A* is 10^8–10^{15} coulomb. Using the lower limit of charge, the coupling constants for electrons α_e and protons α_p near Sgr A*, which has a mass of $M = 4.3 \times 10^6 M_\odot$ according to

GRAVITY Collaboration (2023), are

$$\alpha_e \sim 10^9, \tag{17}$$

$$\alpha_p \sim 10^6. \tag{18}$$

3. Capture Cross-section of Neutral Particles

Before we tackle the main problem, let us find the capture cross-cross section for neutral particles first. Setting $\alpha = 0$, the effective potential V_+ reduces to

$$V_+ = \sqrt{f\left(\frac{\mathcal{L}^2}{\rho^2} + 1\right)}. \tag{19}$$

Capture occurs whenever the particle's energy is greater than the maximum of V_+. The function V_+ is at an extremum when $dV_+/d\rho = 0$ or

$$\rho^2 + (3 - 2\rho)\mathcal{L}^2 = 0, \tag{20}$$

which gives the position of the extrema in terms of $\mathcal{L}$ as

$$\rho_\pm = \mathcal{L}^2 \pm \mathcal{L}\sqrt{\mathcal{L}^2 - 3}\,, \tag{21}$$

where $\mathcal{L} \in [\sqrt{3}\,, \infty)$. When $\mathcal{L} = \sqrt{3}$ ($\equiv \mathcal{L}_{\rm min}$), ρ_+ and ρ_- meet at a saddle point. Inspecting $d^2V_+/d\rho^2$ reveals that ρ_- corresponds to the position of the local maximum of V_+. In terms of $\mathcal{L}$, the escape condition $\mathcal{E} = V_+|_{\rho=\rho_-}$ becomes

$$\mathcal{E} = \sqrt{\frac{2}{27}}\left[\mathcal{L}(\sqrt{\mathcal{L}^2 - 3} + \mathcal{L}) - \frac{3\sqrt{\mathcal{L}^2 - 3}}{\mathcal{L}} + 9\right]^{1/2}. \tag{22}$$

Inverting this equation gives

$$\mathcal{L} = \left[\frac{27\mathcal{E}^4 - 36\mathcal{E}^2 + (9\mathcal{E}^2 - 8)^{3/2}\mathcal{E} + 8}{8(\mathcal{E}^2 - 1)}\right]^{1/2}. \tag{23}$$

The impact parameter b is defined as the perpendicular distance between the center of force and the incident velocity (Goldstein et al. 2001). It can be written as

$$b = \frac{\mathcal{L}}{\mathcal{P}} = \frac{\mathcal{L}}{\sqrt{\mathcal{E}^2 - 1}}, \tag{24}$$

where $\mathcal{P}$ is the specific linear momentum. The maximum impact parameter for capture $b_{\rm max}$ is given by

$$b_{\rm max} = \frac{[27\mathcal{E}^4 - 36\mathcal{E}^2 + (9\mathcal{E}^2 - 8)^{3/2}\mathcal{E} + 8]^{1/2}}{2\sqrt{2}\,(\mathcal{E}^2 - 1)}. \tag{25}$$

The capture cross-section $\sigma_{\rm cap}$ is given by

$$\sigma_{\rm cap} = \pi b_{\rm max}^2 = \frac{\pi}{8}\frac{27\mathcal{E}^4 - 36\mathcal{E}^2 + (9\mathcal{E}^2 - 8)^{3/2}\mathcal{E} + 8}{(\mathcal{E}^2 - 1)^2}. \tag{26}$$

Figures 1 and 2 are plots of $b_{\rm max}$ and the capture cross-section $\sigma_{\rm cap}$ versus $\mathcal{E}$, respectively. For ultra-relativistic particles ($\mathcal{E} \gg 1$),

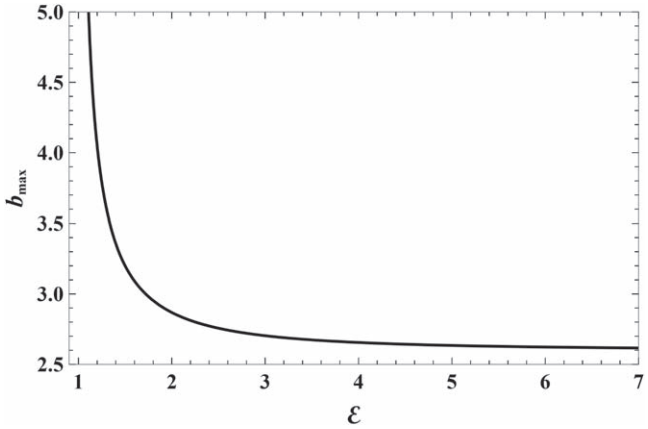

Figure 1. The maximum impact parameter for capture $b_{\rm max}$ vs. $\mathcal{E}$ for a neutral particle.

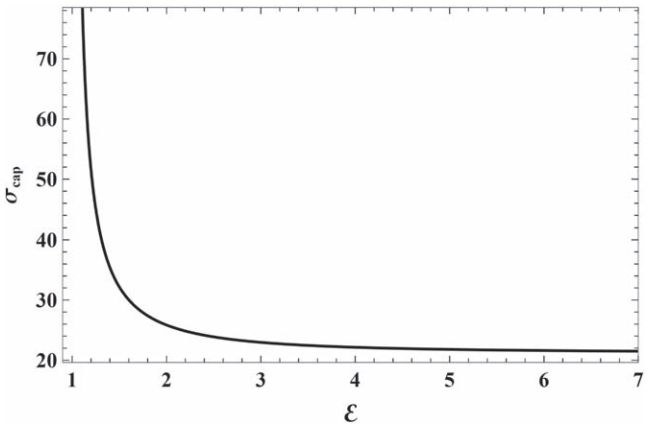

Figure 2. The capture cross-section $\sigma_{\rm cap}$ vs. $\mathcal{E}$ for a neutral particle.

$$b_{\rm max} = \frac{3\sqrt{3}}{2} + \frac{\sqrt{3}}{2\mathcal{E}^2} + \mathcal{O}\left(\frac{1}{\mathcal{E}^3}\right). \tag{27}$$

The corresponding capture cross-section $\sigma_{\rm cap}$ is therefore

$$\sigma_{\rm cap} = \frac{27\pi}{4} + \frac{9\pi}{2\mathcal{E}^2} + \mathcal{O}\left(\frac{1}{\mathcal{E}^3}\right). \tag{28}$$

For a slowly moving particle with speed $v \ll 1$,

$$\mathcal{E} \approx 1 + \frac{v^2}{2}, \tag{29}$$

and thus

$$b_{\rm max} = \frac{\sqrt{2}}{\sqrt{\mathcal{E} - 1}} + \mathcal{O}(\sqrt{\mathcal{E} - 1}) = \frac{2}{v} + \mathcal{O}(v), \tag{30}$$

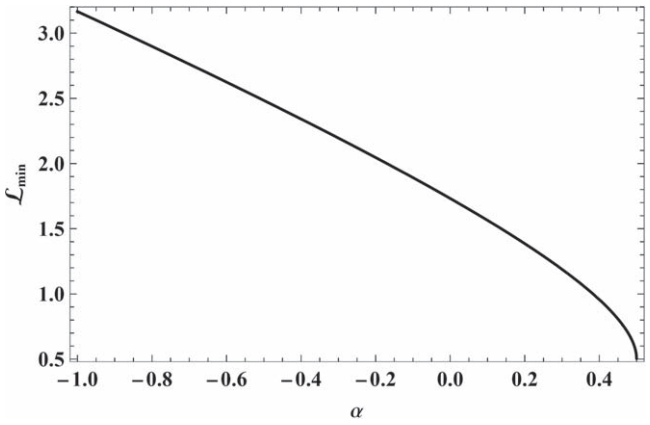

Figure 3. The value of $\mathcal{L}$ at which ρ_+ and ρ_- meet ($\mathcal{L}_{\min}$) vs. the electromagnetic coupling parameter α.

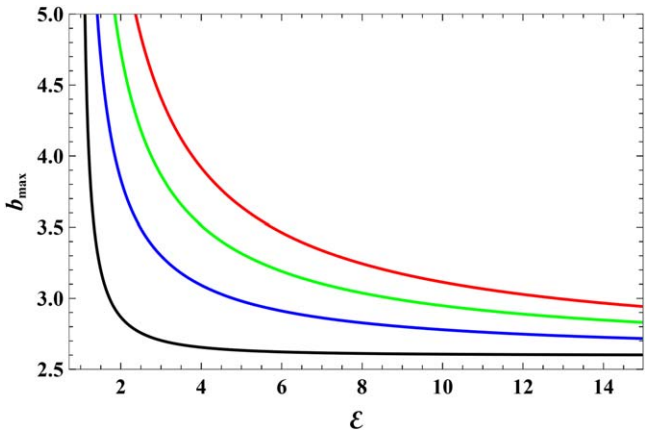

Figure 4. The maximum impact parameter for capture $b_{\max}$ vs. $\mathcal{E}$ for a charged particle with $\alpha = 0$ (black), $\alpha = -1$ (blue), $\alpha = -2$ (green), and $\alpha = -3$ (red).

and the capture cross-section becomes

$$\sigma_{\rm cap} = \frac{4\pi}{v^2} + \mathcal{O}(v^0). \tag{31}$$

4. Capture Cross-section of Charged Particles

We will now follow the same procedure we used for the neutral particle. However, analytic expressions are not viable in this case and we will resort to numerical solutions, except in the ultra-relativistic particle case. The structure of the effective potential V_+ is generically similar to the neutral particle's. The effect of α is to raise (lower) the peak of V_+ for positive (negative) α. The effective potential V_+ is at an extremum when

$$2\alpha\sqrt{(\rho_\pm - 1)(\mathcal{L}^2 + \rho_\pm^2)\rho_\pm} - \mathcal{L}^2(3 - 2\rho_\pm) - \rho_\pm^2 = 0. \tag{32}$$

The extremum is a maximum when

$$\frac{\alpha[\mathcal{L}^2(1 - 2\rho_\pm) + (3 - 4\rho_\pm)\rho_\pm^2]}{\sqrt{(\rho_\pm - 1)(\mathcal{L}^2 + \rho_\pm^2)\rho_\pm}} + 2\rho_\pm - 2\mathcal{L}^2 < 0. \tag{33}$$

To be consistent with the notation of the previous section, we let ρ_+ correspond to the minimum of V_+ and ρ_- correspond to the maximum. Here, $\mathcal{L}_{\min}$ (the value at which ρ_- and ρ_+ meet) depends on the value of α. The two parameters are related by the relation

$$\begin{aligned} -\alpha^8 + 6\alpha^4\mathcal{L}_{\min}^2(\mathcal{L}_{\min}^2 - 3) - 8\alpha^2\mathcal{L}_{\min}^4(\mathcal{L}_{\min}^2 + 9) \\ + 3\mathcal{L}_{\min}^4(\mathcal{L}_{\min}^2 - 3)^2 = 0. \end{aligned} \tag{34}$$

Figure 3 is a plot of $\mathcal{L}_{\min}$ versus α. When $\alpha = 1/2$, $\mathcal{L}_{\min}$ approaches zero. This is because V_+ ceases to have a local minimum for $\alpha \geqslant 1/2$. Physically, this limit corresponds to the case when the Coulomb repulsion becomes too strong for stable orbits to exist as discussed in Al Zahrani (2021).

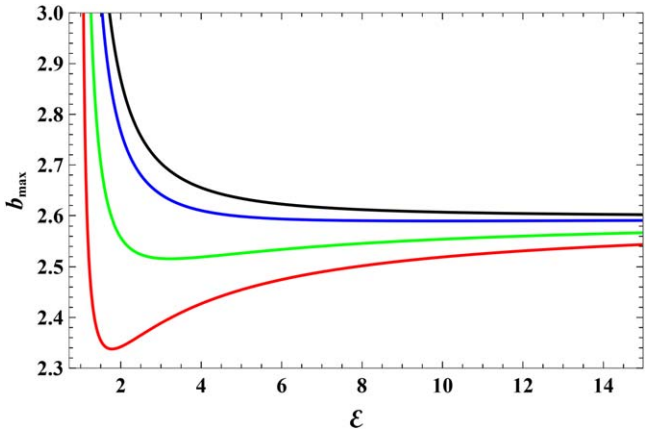

Figure 5. The maximum impact parameter for capture $b_{\max}$ vs. $\mathcal{E}$ for a charged particle with $\alpha = 0$ (black), $\alpha = 0.1$ (blue), $\alpha = 0.3$ (green), and $\alpha = 0.5$ (red).

Figure 4 shows how $b_{\max}$ depends on $\mathcal{E}$ for several negative values of the coupling parameter α. The effect of increasing $|\alpha|$ is to increase the values of $b_{\max}$ for all energies. This is expected because the Coulomb attraction makes it easier for a charged particle to get captured. In all cases, $b_{\max}$ is a monotonic function of $\mathcal{E}$. In the ultra-relativistic limit, $b_{\max}$ approaches $3\sqrt{3}/2$, the limit in the neutral particle case, for any finite value of α, provided that α is not too large compared to $\mathcal{E}$.

Figure 5 shows how $b_{\max}$ depends on $\mathcal{E}$ for several values of α between 0 and 0.5. In this range, there is competition between the gravitational "attraction" and the Coulomb repulsion. The curves have richer structure. They fall quickly as $\mathcal{E}$ goes beyond 1 and reach a minimum. After that, the curves rise and reach $3\sqrt{3}/2$ asymptotically.

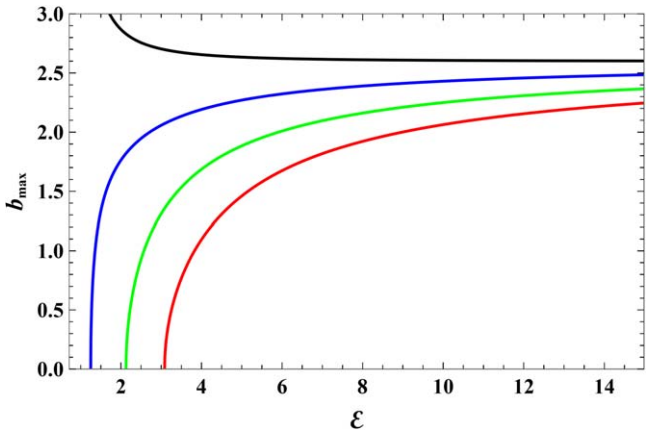

Figure 6. The max impact parameter for capture b_{max} vs. $\mathcal{E}$ for a charged particle with with $\alpha = 0$ (black), $\alpha = 1$ (blue), $\alpha = 2$ (green), and $\alpha = 3$ (red).

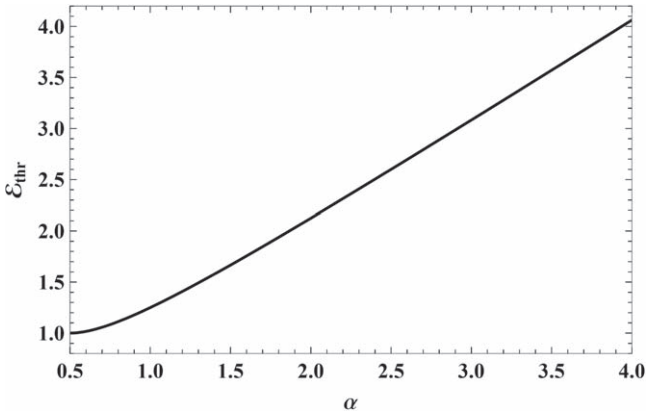

Figure 7. The energy threshold for escape $\mathcal{E}_{thr}$ vs. electromagnetic coupling parameter α.

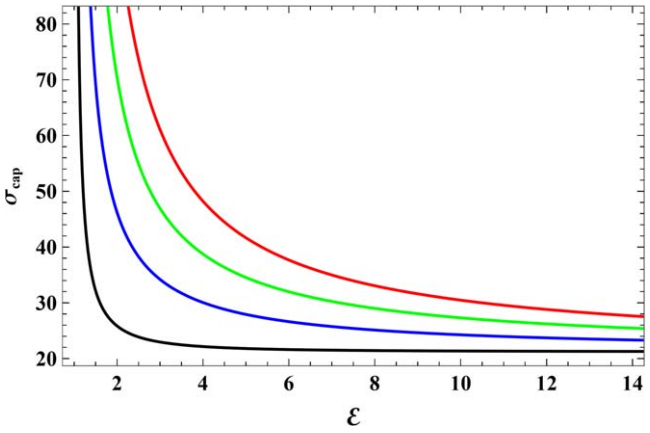

Figure 8. The capture cross-section σ_{cap} vs. $\mathcal{E}$ for a charged particle with $\alpha = 0$ (black), $\alpha = -1$ (blue), $\alpha = -2$ (green), and $\alpha = -3$ (red).

Figure 6 shows how b_{max} depends on $\mathcal{E}$ for several positive values of α greater than 0.5. Generally, b_{max} becomes smaller as α increases. This is expected because the greater the

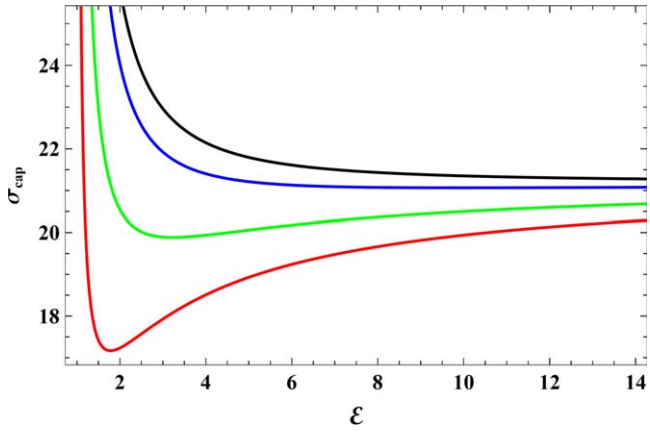

Figure 9. The capture cross-section σ_{cap} vs. $\mathcal{E}$ for a charged particle with $\alpha = 0$ (black), $\alpha = 0.1$ (blue), $\alpha = 0.3$ (green), and $\alpha = 0.5$ (red).

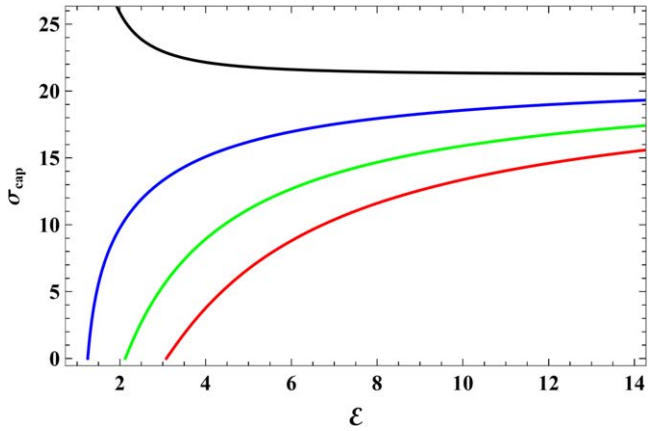

Figure 10. The capture cross-section σ_{cap} vs. $\mathcal{E}$ for a charged particle with $\alpha = 0$ (black), $\alpha = 1$ (blue), $\alpha = 2$ (green), and $\alpha = 3$ (red).

Coulomb repulsion the more difficult it is for a charged particle to be captured. In fact, there is a threshold energy $\mathcal{E}_{thr}$ below which capture cannot occur. It is given by

$$\mathcal{E}_{thr} = \alpha + \frac{1}{4\alpha}. \tag{35}$$

This equation is valid for $\alpha \geqslant 0.5$ only. Figure 7 shows how $\mathcal{E}_{thr}$ varies with α.

The capture cross-section σ_{cap} corresponding to Figures 4, 5 and 6 is shown in Figures 8, 10 and 9, respectively. In all cases, σ_{cap} versus $\mathcal{E}$ curves inherent the features of the b_{min} versus $\mathcal{E}$ curves.

For ultra-relativistic particles, we can write b_{max} as

$$b_{max} = \frac{3\sqrt{3}}{2} - \frac{\sqrt{3}\,\alpha}{\mathcal{E}} + \frac{9 - 2\alpha^2}{6\sqrt{3}\,\mathcal{E}^2} + \mathcal{O}\left(\frac{1}{\mathcal{E}^3}\right). \tag{36}$$

The corresponding capture cross-section is then

$$\sigma_{cap} = \frac{27\pi}{4} - \frac{9\pi\alpha}{\mathcal{E}} + \frac{(4\alpha^2 + 9)\pi}{2\mathcal{E}^2} + \mathcal{O}\left(\frac{1}{\mathcal{E}^3}\right). \tag{37}$$

These limiting results are in agreement with our numerical findings.

5. Conclusion

We have studied the capture cross-section of charged particles by a weakly charged Schwarzschild black hole. We have shown that a trace charge on the black hole can have prominent effects.

When the Coulomb force between a charged particle and the black hole is attractive, it enlarges the capture cross-section significantly. This is expected since the Coulomb attraction enhances the capture of charged particles. However, when the Coulomb force between a charged particle and the black hole is repulsive, it shrinks the capture cross-section significantly. When the electromagnetic coupling strength is below a critical value, capture is possible for all values of the particle's energy. When the electromagnetic coupling strength is above the critical value, there is a minimum value of the particle's energy below which capture is impossible. This is because the Coulomb repulsion surpasses the gravitational attraction unless the particle's radial momentum is large enough.

Our results emphasize the assertion that charged black holes will favorably accrete charges of the opposite sign. However, it is still possible for the black hole charge to grow if the plunging charged particles are energetic enough to the limit that the capture cross-section becomes independent of the sign of the charges. Moreover, the fact that the electromagnetic coupling constant is three orders of magnitudes greater for electrons than protons suggests that it is relatively easier for a black hole to accumulate positive charge than negative charge.

It will be astrophysically interesting to study the energies of charged particles near an astrophysical black hole to understand better how the black hole's charge evolves. The problem can be astrophysically more viable when other astrophysical black holes, such as rotating black holes, are studied (in progress).

ORCID iDs

A. M. Al Zahrani https://orcid.org/0000-0002-5142-6904

References

Ahmedov, B., Rahimov, O., & Toshmatov, B. 2021, Univ, 7, 307
Al Zahrani, A. 2021, PhRvD, 103, 084008
Al Zahrani, A. 2022, ApJ, 937, 50
Anacleto, M., et al. 2023, arXiv:2307.09536v1
Bugden, M. 2020, CQGra, 37, 015001
Carter, B. 1973, in Black Hole Equilibrium States, Black Holes, ed. C. DeWitt & B. S. DeWitt (New York: Gordon and Breach Science Publishers, Inc.), 57
Chandrasekhar, S. 1983, The Mathematical Theory of Black Holes (Oxford: Oxford Univ. Press)
Connell, P., & Frolov, V. 2008, PhRvD, 78, 024032
Frolov, V., & Zelnikov, A. 2011, Introduction to Black Hole Physics (Oxford: Oxford Univ. Press)
Ghosh, S., & Afrin, M. 2023, ApJ, 944, 174
Goldstein, H., Poole, C., & Safko, J. 2001, Classical Mechanics (3rd edn.; London: Pearson)
Gooding, C., & Frolov, A. 2008, PhRvD, 77, 104026
GRAVITY Collaboration 2023, A&A, 677, L10
Kocherlakota, P., et al. (EHT Collaboration) 2021, PhRvD, 103, 104047
Misner, C., Thorne, K., & Wheeler, J. 1973, Gravitation (San Francisco: W. H. Freeman and Co.)
Singh, B., & Ghosh, S. 2018, AnPhy, 395, 127
Tsukamoto, N., et al. 2014, PhRvD, 90, 064043
Young, P. 1976, PhRvD, 14, 3281
Zajaček, M., et al. 2018, MNRAS, 480, 4408
Zajaček, M., et al. 2019, JPhCS, 1258, 012031
Zajaček, M., & Tursunov, A. 1904, arXiv:1904.04654
Zakharov, A. 1994, CQGra, 11, 1027